Maintenance dredging in a macrotidal estuary: Modelling and assessment of its variability with hydro-meteorological forcing

Lemoine J.P. [1, 2, *], Le Hir Pierre [2]

[1] GIP Seine-Aval, Hangar C - Espace des Marégraphes, Quai de Boisguilbert, 76000, Rouen, France
[2] IFREMER, DYNECO/DHYSED, Centre de Bretagne, 29280, Plouzané, France

* Corresponding author : J.P. Lemoine, email address : jplemoine@seine-aval.fr

Abstract :

This study used a hydrodynamic and sediment transport process-based model to simulate maintenance dredging in a macrotidal estuary: the Seine Estuary. This sandy-muddy estuary allows access to two major ports (Le Havre and Rouen). The model accounts for sand and mud dynamics and was previously validated for turbidity and morphodynamic coupling. Dredging is schematised as a physical process responding to simulated seabed evolutions. In coherence with port practices, (i) numerical dredging is conducted when sediment depositions exceed nautical depth limits determined by port authorities; (ii) dredged sediment are released in the water column above dumping sites. The model successfully reproduced the amount of sand and mud dredged in harbors and fairways (7MT/year) without any drift along 10 years. Moreover, the dredged quantities appeared to be considerably higher than the estuarine turbidity maximum (ETM) mass, which was successfully simulated by the model.

The model was used to study relationships between maintenance dredging requirements and hydro-meteorological forcings. Dredging requirements are related to forcings in different ways depending on the exposure of dredged areas to waves, currents and ETM. Le Havre harbor and fairway are sensitive to storms, as 75% of the dredging activity is due to waves higher than 1m. The entrance of Rouen fairway equally responds to tidal range, river discharge and waves. Variabilities in dredging requirements differ depending on the type of sediment. For instance, at the entrance of the Seine navigation channel, mud dredging is strongly correlated to tidal range and secondarily to river discharge, while sand dredging is dominantly related to waves. A specific simulation (not including local wind-induced circulation) showed that the low contribution of waves to mud dredging was explained by materials in suspension hauled off-site. This process is induced by westerly winds that occurred together with waves. On the other hand, mud dredging increases with tidal amplitude in areas of intense tidal currents, and presents a counter clock-wise hysteresis with tidal amplitude, which can be compared to the one followed by the ETM mass. In addition, the dependence of mud dredging on river discharge appears to be related to the proximity of the ETM, the main source of fine sediment, which location shifts downwards when river discharge increases.

At an inter-annual scale, variability in the temporal distribution of hydrometeorological forcings leads to 50% variation of annual dredged masses. In conclusion, this study has improved the understanding of the estuarine dynamics responsible of maintenance dredging.

Highlights

► Maintenance dredging is simulated by a process-based model in a macrotidal estuary. ► Dredging of sand and mud are related to hydro-meteorological forcings differently. ► Dredging needs increase with resuspension either induced by waves or tidal currents. ► Mud dredging is sensitive to the presence of an estuarine turbidity maximum.► Sand dredging varies with river discharge because of the estuarine bottom circulation.

Keywords : Seine estuary, Maintenance dredging, Mud and sand transport, Numerical model - hydrodynamic forcing

1. Introduction

Historically ports were developed in sheltered areas naturally protected from coastal storms, such as estuaries. However these areas are affected by important siltation, requiring maintenance dredging for port activities. Port development and deepening of fairways which occurred in the last 50 years increased the sediment trap effect of harbors and thus the need for maintenance dredging (as illustrated by Byrnes et al., 2011). For international ports, the annual maintenance dredging masses are often counted in millions of tons per year, an impressive example being the Yangtze estuary deep channel where annual dredging volume can almost reach 100 $M.m^3$/year (Liu and Zhang, 2019). This leads to the development of an entire industry: in fact world maintenance dredging cost was estimated in 2011 at 2.5 billions € (IADC, 2011).

Dredging by definition affects environmental functioning by hindering natural morphological evolutions. This impact is all the more important that the related anthropogenic sediment fluxes have similar amplitude as natural fluxes (Zhao et al., 2018). It is the case of the Seine Estuary where annual dredged quantities are i/ of the same order of magnitude as the maritime sediment input, ii/ ten times the Seine River sediment supply (Lemoine et al., 2015). In addition, this anthropization of sediment fluxes alters natural sediment dynamic which can also contribute to enhance the mobility and diffusion of contaminants and pollutants already present in the silted sediments. In this context, and given the increase of marine environmental protection policies, port authorities need to optimize dredging so that their activity remains sustainable either from an economic or from an environmental point of view.

Dredging optimization can mainly be achieved i/ by dredging technique improvement and ii/ by a better understanding of sediment dynamics variability and its implications on dredging. Our research focuses on the latter point and aims to trigger the forcing conditions in which siltation in the dredged areas of the Seine Estuary occurs. In-situ data gathered by port authorities appear to be inhomogeneous over a period of time long enough to assess these dependencies. In fact, field observations variabilities are mainly due to the volume of sediment that can be extracted under given operating conditions. On the other hand, hydro-morpho-sedimentary process-based models have progressed for recent years, becoming more and more realistic, while their computational costs reduced. Since these models allow for considering different forcing, their use for studying relationships between dredged masses and physical forcings is straightforward. This is all the more true as numerical simulations may not account for operational constraints.

Literature about dredging mainly focuses on dredging impact assessment either on morpho-sedimentologic evolutions of the seafloor or on ecological habitat (benthic and pelagic) (e.g. Duclos, 2012; Newell et al., 1998). Among these studies, dredging modelling were mainly

either in sandy environments (*e.g.* Dam et al., 201) or in muddy ones (*e.g.* van Kessel et al., 2015). Literature considering the dredging of sand/mud mixture is poor, but this subject is getting more and more interest as the advance of hydro-morpho-sedimentary models gives access to a knowledge almost inaccessible from in-situ data (Martelo et al., 2019). Nevertheless, to the authors knowledge, no study related to dredging variabilities in response to hydro-meteorological forcing was published, although there might be an abundant grey literature given the strong coastal engineering aspect associated to this subject.

The present work deals with the mouth of the Seine Estuary (France) which is submitted to the maintenance dredging of two major ports, Le Havre Port close to the mouth, and Rouen Port localized more upstream. Within the so-called *Seine-Aval Scientific Program*, a process-based model for hydrodynamics, sediment transport and morphological evolution has been developed for many years (Grasso et al., 2018; Grasso and Le Hir, 2019; Lemoine et al., 2020) and recently upgraded (Mengual et al., 2020). The interest of the modeling approach lies in the possibility to explore many physical processes likely to impact dredging quantities. In particular, the above mentioned model is a 3D process-based model which considers several sediment classes (cohesive and non-cohesive) and their interactions, different transport processes (bed load and suspension) and accounts for multiple hydro-meteorological forcings (tide, river discharge, wind and waves). Consolidation and sediment classes distribution are monitored within a multilayer bed model and morpho-dynamic coupling is respected for both hydrodynamics and wave computations. Moreover, computing performance enables the simulation of long periods, representative of the mid-term natural variability (10 years). Based on the approach proposed by Waeles and Le Hir, (2006) a dredging module was introduced in the Seine Estuary model by Grasso et al. (2018). This module considers dredging as a process responding to simulated morpho-sedimentary evolutions of the sea bed.

Based on the use of a realistic 3D process-based model, this study aims to assess dredging variabilities in response to hydro-meteorological forcings in the macro-tidal estuary of the Seine River. Section two briefly describes the Estuary and the importance of dredging in its functioning. The hydro-morpho-sedimentary configuration of the model is shortly reminded in section 3 together with the validation of dredged quantities with the available in-situ measurement dataset. Section 4 presents the results in term of dredging variabilities and proposes relationship between the Daily Dredged Masses (DDM) and hydro-meteorological forcings. Results and model limits will be discussed in section 5. Conclusions constitute the last section.

2. The Seine Estuary and connected ports

The Seine Estuary, located in the Northern part of France can be classified as a tide dominated estuary (Dalrymple et al., 1992) with a tidal range reaching 8 m at Le Havre. It is 170 km long from the mouth to its upstream limit, the Poses weir. The mean Seine River discharge is 467 $m^3.s^{-1}$ with minimum below 100 $m^3.s^{-1}$ and maximum around 2500 $m^3.s^{-1}$. Salinity gradients and the Estuarine Turbidity Maximum zone (ETM) are located in the lower 50 km of the estuary (area represented on Figure 1). The ETM position and mass are mainly driven by the river discharge and the spring/neap tidal cycle respectively, its mass can reach 250 000 tons during spring tide (*e.g.* Grasso et al., 2018).

As many estuaries, the Seine Estuary was shaped by engineering works to improve the accessibility of marine vessels to Rouen port located 110 km upstream Honfleur (Figure 1), and to Le Havre port close the mouth (*e.g.* Avoine et al., 1981; Lesourd et al., 2003). In particular, two submersible dikes, almost 10 km long, were built in the 1960's (dashed lines on Figure 1). These dikes were designed to enhance ebb currents and thus to limit siltation in

the navigation channel, located between these dykes (*e.g.* Le Hir et al., 2001). Navigation channels of both Rouen and Le Havre port were significantly deepened to -6.3 m and -15.5 m below lowest astronomic tide, respectively. These engineering works induce extensive maintenance dredging in order to maintain a constant nautical depth in both fairways.

Rouen navigation channel stretches from Honfleur to Rouen, but most of its maintenance dredging activity is located in the lowermost 20 km of the estuary (85%). In this downstream estuary, more than 90% of the dredged mass is extracted in two areas: one is located at the seaward end of the submersible dykes, and for this reason is named with the French word "engainement" (hereafter mentioned as *zone E,* Figure1), while the other is 20 km upstream, right south of a breach in the northern dyke where intense sediment exchanges occur between the northern channel and the navigation channel (Delinares et al., 2015), and is called *zone B* hereafter (Figure1). Characterized by strong tidal currents reaching 2 m.s^{-1} on spring tides, these two areas respectively correspond to the extreme seaward position of the Seine ETM and to its central position (Grasso et al., 2018). Dredging upstream from Tancarville is not in the scope of the present study.

Despite strong local hydrodynamics and currents exceeding 2 m.s^{-1}, siltation in this part of the navigation channel of Rouen Harbor is important. Around 2 million tons of sediment, equally composed of sand and mud, are dredged each year in *zone B* while in *zone E,* the dredged material is sandy mud (65% in weight) and amounts to 3 million tons. Dredging of Rouen port is operated continuously by at least one trailing suction hopper dredger. Prior to 2017, these sediments were released on a disposal site called Kannik, located just at the mouth in a very dynamic area (Figure1). Nowadays these sediments are dumped more offshore (see section 3.3).

Le Havre port is dredging an annual volume of around 2 million tons in its basins and navigation fairways (hereafter called *zone LH*). As tidal currents are low in these areas, and as waves remain moderate in the deep navigation channels, sediment dredged is mainly muddy (90% of mud). These sediments are released on the disposal site of Octeville located north from the mouth of the estuary (Figure 1). Sediment dumped on both Kannik and Octeville are likely to be partly redistributed towards the estuary.

Analyzing the actual sediment budget of the Seine Estuary and confronting natural sediment inputs to the annually dredged masses shows that the total dredged mass (7 million tons) is much higher than the continental sediment input (0.55 million tons per year; Landemaine, 2016) and has the same order of magnitude as the marine natural sediment input (4 million tons per year estimated from bathymetric surveys; Avoine, 1995)).
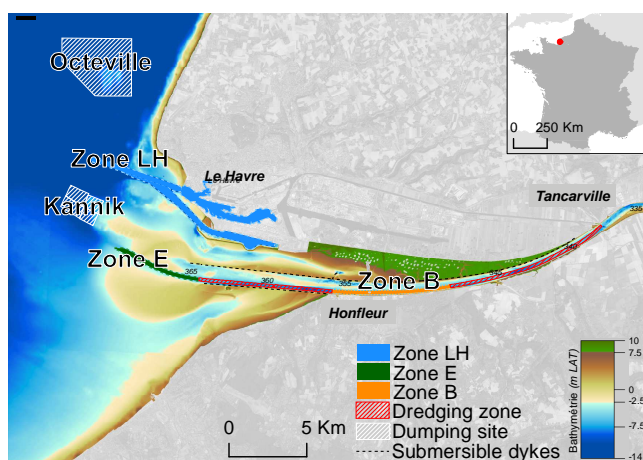
Figure 1 : bathymetry of the area of interest with dredging and dumping areas and submersible dykes. The dredged zones LH, E and B are represented in blue, green and orange respectively. Other dredged zone are represented in hatched red.

3. Material and methods : The hydro-morpho-sediment model of the Seine Estuary

Our approach relies on the use of the hydrodynamic model MARS-3D (Lazure and Dumas, 2008), coupled to the process based morpho-sediment model of Le Hir et al. (2011). A detailed description of the model set-up and the validation of both hydro and sediment dynamics can be found in Grasso et al. (2018). This model of the Seine Estuary was also used by Grasso and Le Hir (2019) to study the influence of morphological changes on suspended sediment dynamics in the Seine Estuary from 1960 to 2010.

Recently, Mengual et al., (2020) updated the sediment model mainly regarding three points:

- explicit computation of bedload fluxes, accounting for slope effects,
- improved management of sediment resuspension in the non-cohesive regime,
- better representation of porosity in sediment layers, depending on grain sizes.

For the needs of our study, this new version of the model was fitted and a dedicated calibration was sought in order to reproduce the siltation observed in the navigation channels without compromising the validation level demonstrated by Grasso et al. (2018). Sediment is dredged and dumped according to specific rules given by port authorities. Main model characteristics are shortly reminded in sections 3.1 (hydrodynamics) and 3.2 (sediment dynamics), while detailed can be found in Mengual et al. (2020). The methodology for computing sediment dredging and release is detailed in section 3.3. Characteristics of the simulated period are described in section 3.4. Finally, validation of dredging results is presented in section 3.5.

3.1. Hydrodynamic models

The MARS-3D flow model solves the Navier-Stokes equation under hydrostaticity assumption and Boussinesq approximation, using a finite difference method (Lazure and Dumas, 2008). The model runs on a curvilinear non-orthogonal grid in order to have boundary conditions farther without increasing computation time and also to fit the shape of the estuary. Grid resolution ranges from 2x2 km^2 in the bay of Seine to 30x100 m^2 in the estuary mouth (area of interest). The 10x10m bathymetric data acquired in 2009 and provided by port authorities of Rouen and Le Havre were interpolated on this grid (Figure 2). The vertical discretization compounds 10 sigma layers equally distributed.
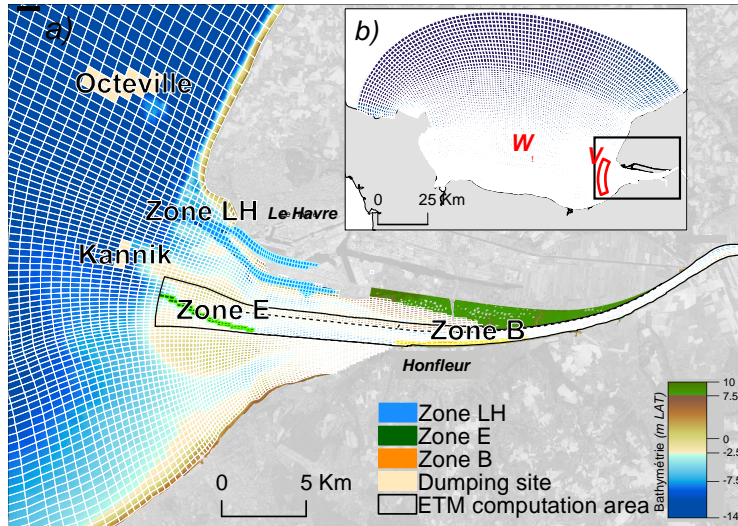
Figure 2 : Computational grid and bathymetry of the Seine Estuary numerical model and zoom in the area of interest for this study (a) and in the bay of Seine (b). Cells of the three dredged zones (LH, E and B), studied in section 4 are represented in blue, green and orange resp. Cells of the dumping sites Octeville and Kannik are represented in beige. Cells considered to compute the ETM dynamics according to Grasso et al. (2018) are surrounded by a solid black line. On the bay of Seine map (b), the area designated by letter V represents the area considered to define wave data (cf. 2.4). Point W corresponds to the location of the wind data used in section 4.

The hydrodynamic model is forced by realistic tidal components at its northern open boundary. Diurnal Seine River and intra-estuarine tributary discharges are imposed at their confluence with the estuary. Meteorological forcings are constituted by wind and pressure gradients resulting from the AROME model developed by Meteo-France (Seity et al., 2011). Waves are simulated by the WaveWatch III code which is coupled to the MARS-3D flow model. The wave model is locally forced by the same wind information than MARS3D within the domain and by results from a large-scale model of the Atlantic Ocean along the open boundary (Roland and Ardhuin, 2014). In return, WWIII model provides to MARS-3D the parameters needed to compute the wave induced skin stress τ_w , following the Jonsson, (1966) formulation with a wave friction factor f_w expressed according to Soulsby et al. (1993). The computation of wave plus current bottom shear stress follows Soulsby (1997). In order to account for morpho dynamics coupling, bathymetry is regularly updated in the circulation model and in wave computations. To improve the feedback of sediment evolution on sediment resuspension and mixing, a variable skin roughness length z_0 is used. It depends on the simulated representative diameter of the non-cohesive fraction of surficial sediments $D_{gravsan}$, $z_{0\ skin\ (m)}= \max(D_{gravsan}/15, 10^{-5})$; the minimum value ($10^{-5}$ m) is defined in accordance with the finest sand class, and is also used in case the surficial sediment is cohesive]. The form bottom roughness length $z_{0\ form}$ used for computing the bed shear stress in the momentum equation is also dynamic and directly proportional to the averaged diameter of non-cohesive sediment within the first centimeter of the sediment ($D_{gravsan1cm}$, updated by the multi-class sediment model), using the following relationship: $z_{0\ form\ (m)}= K_{z0}.D_{gravsan1cm}$, where K_{z0} is a calibration coefficient (set at 3.5) that accounts for the probable occurrence of bedforms.

3.2. Sediment model

The hydrodynamic model is coupled to the process-based sediment model for sand and mud mixtures MUSTANG (MUd Sand TrANsport modellinG) (Grasso, 2015; Le Hir et al., 2011; Mengual et al., 2017; Mengual et al., 2020). This multi-class sediment model computes both

transport in suspension and bedload for different sediment classes ranging from mud (only transported in suspension) and sand (transported in suspension and as bedload) to pebble/gravel (bedload only).

As detailed in Mengual et al. (2020) the model simulates bedload according to Wu and Lin (2014) and distinguishes the three erosion regimes described in Le Hir et al. (2011): non-cohesive, transition from non-cohesive to cohesive, and cohesive, depending on the surficial mud fraction. The threshold mud fraction between non-cohesive and transition increases with the averaged non-cohesive sediment diameter to represent the decreasing ability of the mud to impede sand or gravel movement. In order to better fit field and experimental observations, a transition varying exponentially with mud fraction was introduced (Mengual et al., 2017). Slope effects on fresh sediment deposition are also considered using a schematic approach which consists in transferring a fraction of the depositing material into adjacent computation cells proportionally to the bottom slope. Such slope effect appears to play a significant role on deposition in deep channels and consecutive dredging, as in *zone LH.*

Suspended sediment transport is simulated by solving an advection/diffusion equation for different sediment types ranging from mud to fine and medium sand (Le Hir et al., 2011). Flocculation processes are accounted for by a variation of the mud settling velocity with mud concentration and turbulent intensities, following Van Leussen (1994). In the application to the Seine Estuary, five representative classes of sediment are considered: one "mud", three "sands" (100, 210 and 800 µm) and one "gravel" (10 mm). These classes have been selected from dominant sizes observed in the area (see also Grasso et al., 2018).

A multi-layered bed model is associated to the hydrodynamics model, with the same horizontal computation grid. The vertical discretization of the sediment enables to account for the variable sediment distribution and consolidation processes. Layers thickness varies according to erosion and deposition events, between a minimum value (1 µm) and a maximum (5 mm), so that changes of sediment composition can be preserved. In case deposition in excess implies an increase of the number of layers above a maximum (100 in the present application), a buffer layer with unlimited thickness is constituted at the bottom of the sediment. Consolidation of sand and mud mixtures is solved according to a modified Gibson equation (Grasso et al., 2015).

The initialization of sediment constitutes a major input of the model, as sediment dynamics depend on the surficial sediment characteristics. Initializing sediment means setting its thickness, the 3D distribution of the five sediment classes, and the spatial distribution of porosity. For the sake of simplicity, a uniform vertical distribution of sediment classes is assumed, together with a vertically uniform porosity. Similarly, a uniform thickness of 3 m is considered, based on the maximum erosion which is likely to occur in the mouth of the Seine Estuary, along a 10 years simulation. Then the adopted strategy for the horizontal distribution of initial sediment is twofold. In the large area of the Bay of Seine, where sediment is mainly coarse sand due to strong tidal currents, the time scale to get an equilibrium sediment cover from a uniform distribution is supposed to be very long. It is then assumed that the initial sediment reflects the bottom shear stress gradients. A positive relationship between the range of higher shear stresses (percentile 80 of the current induced shear stress along a whole year) and typical sediment facies (from fine to coarse) is assumed, and fitted to field samples compiled by Vaslet et al. (1978) (in Blanpain, 2009). On the other hand, in the small and highly dynamic area of the estuary, a uniform sediment cover is preferred, following the proof of concept published by Grasso and Le Hir (2019) who showed that the model could simulate a realistic sediment cover after a spin-up period of one year. After some trial and errors tuning, the initial sediment in approximately the area zoomed in Figure 2 (*i.e.* the whole area of interest) is composed of 40% mud, 60% sand (100 µm: 15%, 210 µm: 30%, 800 µm: 15%) and 5%. In addition, areas known to be non-erodible are initialized without

sediment in order to prevent excessive local erosions and their possible morphodynamic consequences.

Continental sediment supply from the Seine is imposed at the upstream limit of the model: a relationship between river discharge and suspended solids concentration (SSC) is assumed, based on Avoine et al. (1981). Although low, the sediment supply from intra-estuarine tributaries is also considered using the model proposed by Landemaine (2016). More essential for long term simulations, water masses entering the computational domain from the open sea may be slightly turbid, inducing non negligible input as water fluxes are considerable there. A constant and uniform concentration of mud equal to 2 mg.l^{-1} is imposed at the ocean open boundary, qualitatively in agreement with observations in the English Channel, as described by *e.g.* Blanpain (2009).

3.3 Dredging procedure

One original feature of our model is not to force dredged quantities provided by observations, but to simulate them according to the same rules as in real life: typically, when deposition makes the sediment exceed nautical depth, the deposited mass in excess is removed and released in the water column above the dumping sites (Lemoine et al., 2020). Nevertheless, it should be noted that dredging is operated continuously in all maintained areas in the model, while it depends on the dredger availability in reality.

Three dredging rules were defined to schematized dredging as it is operated by port authorities. The first rule is the nautical depth which can be specified for each dredged area. A second rule is the minimum sediment density considered to define the nautical depth. As bathymetric surveys in the Seine Estuary are conducted using a 33 kHz sonar which cannot measure mud deposition below 300 kg.m^{-3}, this concentration was considered as a threshold to compute the sediment thickness. The third rule is related to the "nominal" dredged thickness: it corresponds to the sediment depth concerned by a dredging operation. In our application, this thickness does not include the height of unconsolidated sediment (*i.e.* < 300 kg.m^{-3}, *cf.* rule 2), so that when a cell is dredged, the total dredged height is equal to the sum of the nominal dredged thickness and the surficial unconsolidated sediment. Our realistic run considers a nominal dredged thickness of 50 cm in accordance with real dredging practice. Nevertheless to assess dredging variabilities regarding hydrometeorological forcings and especially to minimize the delay between the sediment influx induced by any forcing and the actual dredging operation, a specific simulation was set up, with a nominal dredged thickness of only 1 cm. Comparisons between this so-called quasi-continuous dredging run (*QCD* run, dredged thickness =1 cm) and the realistic one (dredged thickness = 50 cm) will be specifically discussed in section 4 (results).In addition, the form bottom roughness length z_0 $_{form}$ is fixed (0.1 m) in dredged areas, in order to account for a roughness enhanced by dredgers.

Following these rules, sediment is removed from the sea bed of dredged areas when the bed elevation exceeds the nautical depth specified by port authorities. Then it is instantaneously released above the dumping site of Kannik (resp. Octeville) for sediment dredged by the port of Rouen (resp. Port of Le Havre). In coherence with results from Nguyen et al., (2012), gravel is released on the sea floor while sand and mud are released in suspension uniformly in the lower half of the water column where they experience the same dynamic as the background suspension. During the release process, deposition is affected by the hydrodynamic conditions and especially turbulence. If dumping is occurring at slack tide, with low level of turbulence, most of the released sediment deposits. On the contrary during the ebb or flood, the net deposition rate is lower and a larger part of dredged sediment remains in suspension.

Results of the dredging procedure are stored as time series of dredged masses of each class of sediment (mud, sands and gravel) per dredging area, with a period of 2 hours.

3.4. Characteristics of the simulated period and forcing data

A spin-up period of 1 year, corresponding to the actual forcing of year 2009 is first conducted without morphological coupling to preserve the initial bathymetry. This spin-up initiates the estuarine sediment dynamic, redistributes sediment to get a more realistic surficial sediment cover and builds up a representative estuarine turbidity maximum. Then the model is re-started on January the 1st, 2009 with initial conditions corresponding to the end of the spin up period. 2009 results presented hereafter correspond to the first year after the spin-up period.

Results shown hereafter come from retrospective simulations starting in January 2009 and ending in December 2018. This 10 years period covers the whole range of variation of the considered forcings. Seine River discharges over this period are characterized by a low run off equal to 146 $m^3.s^{-1}$ (percentile 1), a high run off of 1600 $m^3.s^{-1}$ (percentile 99), and a median (resp. average) one of 354 $m^3.s^{-1}$ (resp. 477 $m^3.s^{-1}$). This is fully representative of the variability over last 50 years which are characterized by a first percentile of 110 $m^3.s^{-1}$, a last percentile of 1647 $m^3.s^{-1}$ and a median value of 354 $m^3.s^{-1}$ (average: 467 $m^3.s^{-1}$). Similarly, the whole range of variation of wind and wave regimes can be observed during the 10 years of this simulation. It can be noted that year 2018 is characterized by the occurrence of a very high run off reaching 2120 $m^3.s^{-1}$, and a strong storm with waves of 3.6 m at the entrance of Le Havre port.

Dredging variability will be assessed in regard to four forcings: river discharge, tide, waves, and winds. Seine River discharges and tidal data correspond to the model inputs (*cf*. 2.1). Waves data were extracted from our simulation as a spatial average over the zone V presented on Figure 2. Wind data used for the comparison were extracted at point W (Figure 2) from the Meteo-France AROME model used to force our hydrodynamic and wave models.

3.5. Model Validation

Hydro-sedimentary validation of the model in term of water level, wave propagation, SPM dynamics and morphological evolutions is provided in Grasso et al (2018) and Mengual et al. (2020). However, the few adjustments operated on bottom friction coupling (section 3.1) have slightly modified some validation scores. For instance, although the tide propagation and attenuation remains well simulated up to the upstream limit of the estuary, the squared correlation coefficient on tide elevation is 0.99 instead of 1 and the root-mean-square error 0.31m instead of 0.15 m in the estuary mouth when compared to Grasso et al. (2018) results. Waves validation is similar to previous results (root-mean-square error of 0.2 m on H_s; Grasso et al., 2018).

Suspended sediment concentrations had been thoroughly validated by Grasso et al. (2018), but a slight change of parameterization had been introduced by Mengual et al. (2020) in order to get a better agreement on morphological changes at the time scale of several years (see also Grasso et al., 2020). As a result, the agreement between the model and observed bathymetric evolution is quite reasonable: when splitting the 150 km^2 of the mouth into 7 boxes, model results and observations can be compared in terms of global sediment accretion or erosion: only one box shows opposite results. Among the other ones, four are in erosion (total observations: 19.3 Mm^3, total simulations: 17.5 Mm^3), while two of them

experience accretion (total observations: 19.9 Mm^3, total simulations: 13.7 Mm^3). The drawback of this morphological performance is some degradation of the suspended matter concentration, which becomes underestimated. While the normalized root-mean-square error was between 0.2 and 0.4 in previous modeling when computed on one year comparison in three locations (Grasso et al., 2018), it is now in the range 0.3 - 0.6 in our modeling and the normalized bias is about -0.5 in the area of interest (Grasso et al., 2020).

Validation results presented here mainly highlight the capacity of the model to reproduce dredging variabilities.

Port authorities of Le Havre and Rouen provided both qualitative and quantitative information to validate model dredging results. Considering the important variabilities induced by human and technical constraints, reference for in-situ data were established as yearly-averaged mass of dredged sand and mud. Higher frequency data and even yearly quantities are more influenced by the availability of dredging ships than by a variability of needs for maintenance dredging.

In the downstream part of Rouen fairway, dredging is operated along 32.3km but 94% of the dredging is done along the 13.1km corresponding to *zones E and B* (Figure 1). Model results present a good agreement with this distribution, since 88% of the numerical dredging is also achieved in *zones E* and *B*. As for the dredging zones of Le Havre port and fairways, given their simple schematization in the model, and for the sake of clarity, they have been compiled in a unique compartment "*zone LH*". Validation and results will therefore relate to these 3 zones : *zone LH, E and B*.

3.5.1 Composition of dredged sediments

Dredged masses are routinely measured and recorded by the trailing suction hopper dredgers which operate in the Seine estuary . Sediment grain size is not routinely measured but some measurements were done between 2008 and 2009 by Rouen port. Samples were not collected directly on the seafloor but between the suction pipe and the hold of the dredger, so that the resulting mud fraction can be expected to be somehow underestimated. Figure 3 represents the average grain sizes observed and computed for the dredged *zone E* (panel a) and *B* (panel b) . At E, *in-situ* and computed dredged sediments have nearly the same composition. The highest difference concerns very fine sands which tend to be underestimated by our model. At B model results also present a fairly good agreement with observations, with some underestimation of sand classes that will be discussed further.
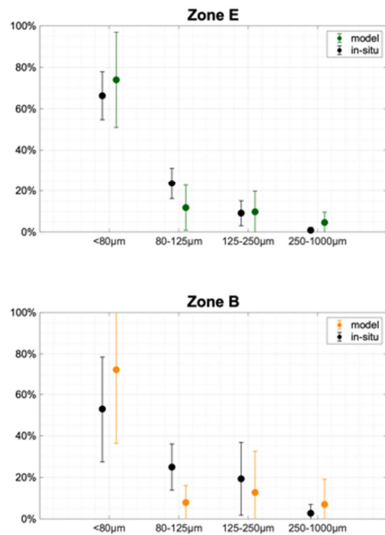
Figure 3 : Grain size comparison between in situ data and model results averaged over the 10 years period in zones E (a) and B (b).

For *zone LH*, the only data provided by port authorities are an average mud fraction of 88% over the years 2007 to 2014. The simulated mud fraction in sediment dredged in *zone LH is* 92% on average, quite in agreement with observations.

3.5.2 Quantification of dredged sediments

In the following, the model capacity to reproduce dredging in the three main dredging zones is evaluated regarding the yearly dredged masses of mud and sand (Figure 4).
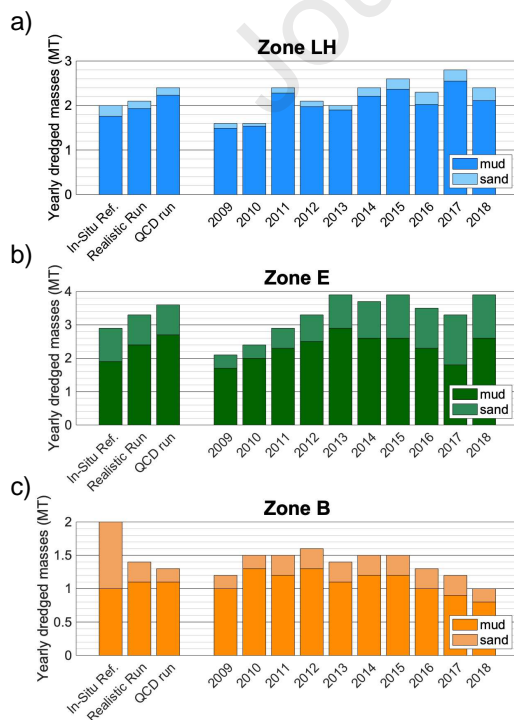
Figure 4 : Comparison of yearly dredged masses of mud and sand between in-situ reference and model results for the reference run over the simulated period (from January 1st 2009 to December 31st 2018), on the three main dredged areas Zone LH (a), Zone E (b) and Zone B (c). First column represents the in-situ reference, while the second and third column represent the results of simulations averaged over 10 years for the realistic and QCD runs respectively. The other 10 columns represent the yearly results of the realistic run.

For *zone LH*, model results (2.2 Mt with 92% of mud on average) are quite in agreement with *in situ* reference data provided by port authorities (2 Mt with 88% of mud). However, regarding the known interannual variability of ±0.4 Mt (Le Havre Port Authorities, *pers. comm.*), simulated dredged masses seem to increase a bit too much along the simulated period. Regarding the mud content, there is a good agreement between *in situ* data and model results. It is concluded that results in *zone LH* are representative of the reality.

Zone E reference is set at 2.9 Mt of sandy mud (65% of mud content) with a variability of almost 1Mt depending on the yearly regime of hydro-meteorological forcing. Model results on this site (Figure 4) are satisfactory, with a mean computed dredged mass equal to 3.3 Mt of sandy mud (72% mud content). On this site the model seems to be able to reproduce the inter-annual variability as qualitatively reported by port of Rouen.

Model results on *zone B* are not as good as on the two other sites (located downstream). The sand deposition calculated in this area seems to be underestimated by a factor 2 in our model. This may be due to some underestimation of sand exchanges between the northern channel and the navigation channel through the breach. Except from this, mud deposition is well reproduced.

On a daily scale the daily dredged masses in the model can reach 30,000t/day for each of the two ports (Figure 5).These quantities are compatible with the dredging capacity of the two ports whose vessels operate 24 hours a day, 7 days a week. For example, the dredging vessel "Samuel de Champlain" has a carrying capacity of 13,000t.

Averaged results over the ten years period are similar in the *realistic* run (with 50 cm dredged thickness) and the *QCD* run (with 1 cm dredged thickness). Nevertheless both local dredged masses and mud ratios present a better agreement with *in-situ* data in the realistic case (Figure 4). Differences between these two runs will be further discussed in section 4.2.

An interesting result of these simulations is the ability of the model to simulate and maintain a realistic ETM over 10 years (Figure 5). In particular, the simulated ETM dynamic remains steady and its seasonal variation is in accordance with results over an hydrological year showed by Grasso et al. (2018). In particular, the dependence of the ETM mass on the tidal range is clearly visible. Integrated over the same area as the one proposed by Grasso et al. (2018) and reminded in Figure 2, the simulated ETM mass is 40 kt in average, slightly lower than the one (48kt) computed by Grasso et al. (2018).

Overall, dredging validation is satisfactory in terms of quantities of both mud and sand over the decadal period. Considering dredging as one of the validation criteria for modeling sediment transport, it can be noted that our model is able to reproduce mid-term sediment dynamic without any distortion of the SPM dynamics. This level of validation allows a thorough analysis of relationships between dredging and the intensity of different hydro-meteorological forcings, as developed in section 4.

4. Dredging variabilities and relations with hydro-meteorological forcing

4.1. Temporal variabilities

Beyond the indicators used to validate the model, the outputs over the simulated 10 years period offer a rich spectrum of information to evaluate dredging variabilities and responses to natural forcings (Figure 5).

Firstly, the model reproduces the continuous dredging needed to maintain nautical depths. In coherence with in-situ data and model results presented in Mengual et al. (2020), this fact illustrates that these zones of the estuary are prompt to accretion while the morphological evolution over the whole estuary appears to be in a quasi-equilibrium at this time-scale (ARTELIA, 2018). This continuous siltation might be favored by maintenance dredging itself, as the latter prevents local morphological evolutions. Thus by inhibiting a possible equilibria, maintenance dredging also maintains the sediment trapping character of over-deepened channels.
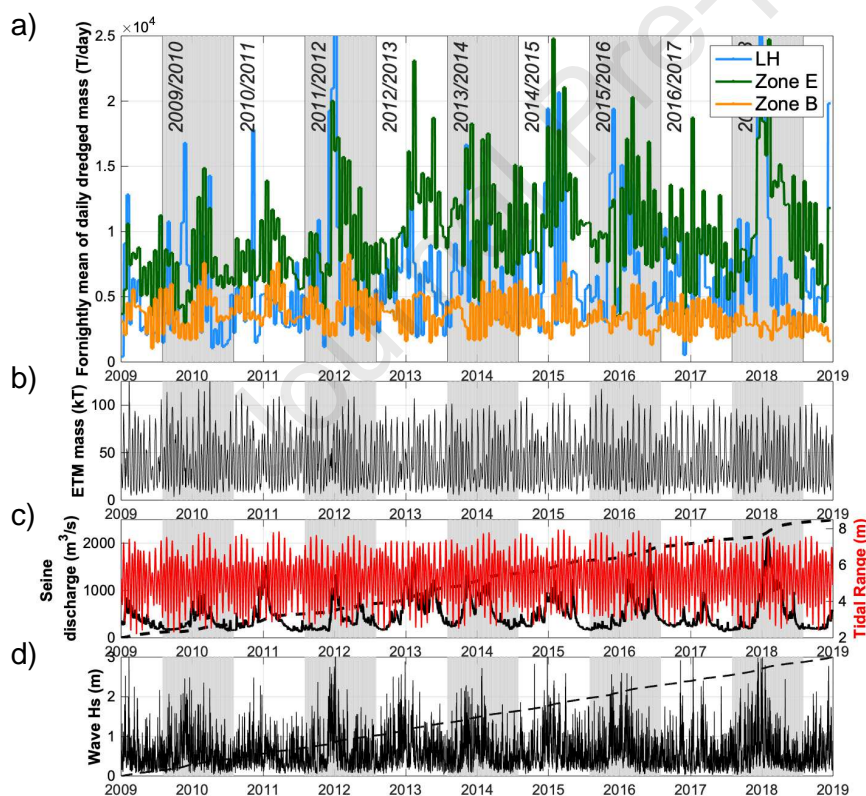

Figure 5 : Chronological overview of the dataset from January 2009 to December 2018: fortnightly averaged dredged masses for zone LH, E and B (a), ETM mass calculated in the area specified on Figure 2 (b); tidal range and river discharge (daily and cumulated) (c), and waves Hs (hourly and cumulated) (d). Cumulated river discharge and cumulated wave Hs were scaled to reach maximum of their respective daily data. The alternance of grey and

white areas in the background highlights each hydrological years (from august 1ˢᵗ to July 31ˢᵗ).

Over the decadal period presented on Figure 5, daily dredged quantities present important variations. Periodic increases of dredged material correspond to winter periods when the system is dynamic.

Figure 6 presents a zoom over the period august 2017 to august 2018. Relations between dredging and forcings can be perceived from the comparison of the dredged activity on panel a, b and c with the intensity of the forcings on panel d, e and f. At this scale the tidal induced variability of DDM is highlighted. For *zones LH and E*, this cyclicity in the DDM appears to be modulated by a seasonal variation, related to higher river discharge but also more frequent winter wave events. Compared to these two areas, *zone B* appears to be less sensitive to this stormy period and dredging there remains mainly driven by tidal variabilities.
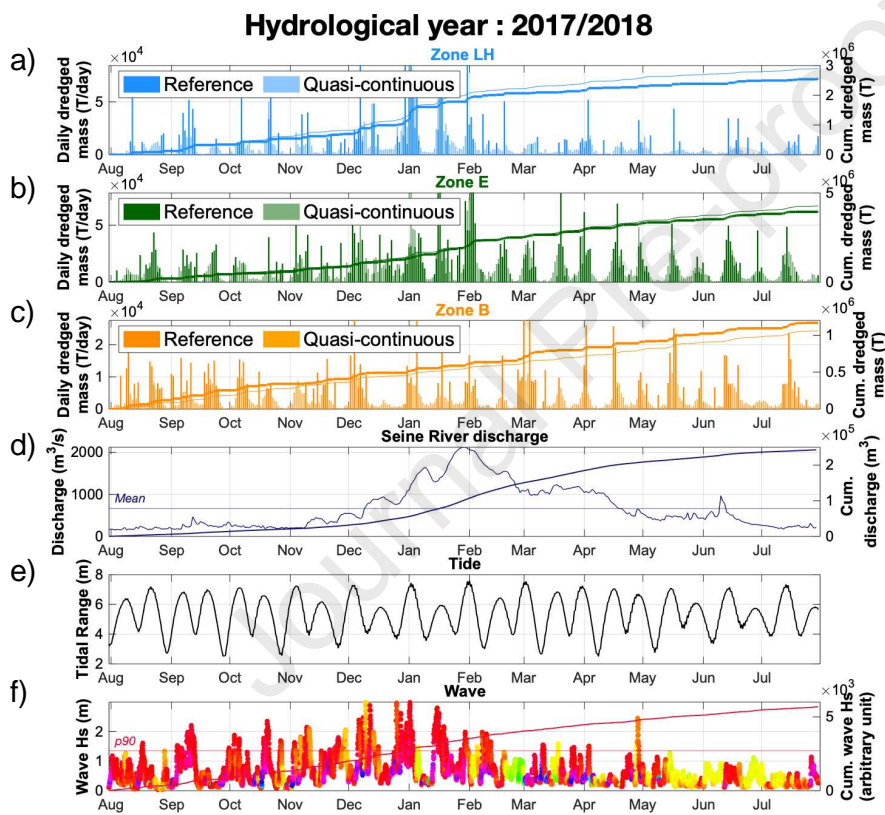

Figure 6 : Daily and cumulated dredged masses along the hydrological year 2017-2018 for the 3 sites zone LH (a), zone E (b) and zone B (c) together with daily and cumulated river discharge (d), tidal range (e) and hourly wave significant height Hs (f). Wave directions are represented by colors as indicated in the circular legend of Figure 8, and the cumulated sum of wave Hs is superimposed on the wave plot in order to highlight seasonal trends. Daily and cumulated dredged masses are provided for the reference run (dark color) and the quasi continuous run (light color).

4.2. Comparison of the Realistic run and quasi-continuous dredging run

The realistic run differs from the *QCD* run by only one parameter value: the dredged thickness of consolidated sediment (*i.e.* > 300 kg.m^{-3}). In the realistic run dredging is conducted realistically by layers of 50 cm while in the *QCD* run it is operated by layers of 0.01 m, thus more frequently. Results of both runs over 10 years are comparable. Nevertheless, dredging quantities of both sand and mud present a better agreement with field data in the realistic case.

Figure 6 presents results of both realistic and *QCD* runs in terms of dredging over the hydrological year 2017/2018. As anticipated, DDM variability is much smoother and more responsive in the *QCD* case than in the realistic run. Interestingly, cumulated dredged masses are slightly larger with the *QCD* run for *zones LH and E* but not for *zone B*. Actually *Zone B* is more upstream and protected from the waves. The downstream zones, which are exposed to waves, might receive transitory sediment deposition, a part of which is likely to be naturally eroded before a thickness of 50 cm has been reached, which would not be the case in the quasi-continuous dredging run. On the contrary, the larger dredged mass observed on *zone B* in the reference run might be explained by a stronger trapping effect induced by the 50 cm hole constituted after dredging, which does not happen in the QCD procedure.

These observations reveal the limited effect of the dredged thickness on sediment dynamic in the vicinity of dredged areas. In fact, in the realistic case there could be either i/ more dredging as removing a rather large thickness of sediment generates a more effective sediment trap or ii/ less dredging as dredging is operated less frequently, increasing the quantities of few consolidated sediment which can be eroded naturally by strong currents (instead of being dredged).

Overall, the QCD procedure minimizes the accretion needed to trigger dredging and thus enables a better estimation of the relation between the hydrometeorological forcings and dredging. Therefore the quasi-continuous dredging run is used hereafter.

4.3. Dependence of daily dredged sediment mass and composition on hydro-meteorological conditions

To better estimate relationships between DDM and forcings, each DDM (or fortnightly averaged DDM) and its associated mud fraction can be correlated to each forcing (Figure 7). Regarding the Seine River discharge, which is measured upstream of the Seine Estuary, and considering the time lag between the river discharge at the measurement location and the response of the estuarine system, especially at the mouth, it has been chosen to average both DDM and river discharge over a period of 14 days. This time averaging filters out the fortnightly tidal variations, and also corresponds to some mean value of the river flow propagation time along the estuary. On the opposite, for investigating responses to tides, each daily dredged mass is considered, in order to characterize the tidal range, and even distinguish periods from neap to spring and spring to neap. By this way a possible hysteresis generated by the delay of deposition after resuspension by spring tidal currents can be sought. Last, for the wave forcing, the maximum wave Hs during the same day as DDM was selected. Considering river discharge and waves height, it is important to keep in mind that there are few occurrences of extreme values (e.g. discharge > 1250m^3.s^{-1} and wave Hs > 2 m), so that uncertainties associated to these ranges are higher.

4.3.1. River discharge

Regarding the Seine River discharge, a strong variability is observed but a global DDM increase with discharge can be seen for *zone LH and E.* In addition mud fraction seems to slightly decrease with river discharge: this topic will be further discussed in 4.4. In *zone B,* DDM slightly decreases with river discharge.
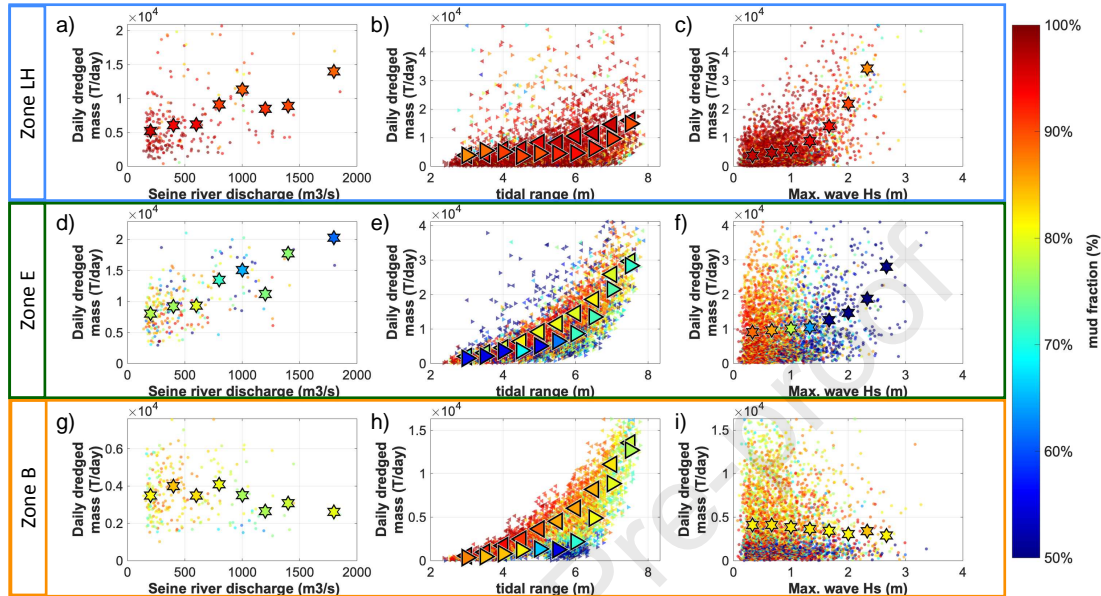

Figure 7 : Daily dredged mass (DDM) and associated mud fraction (color) in response to river discharge, tidal range, and wave conditions for the three zones: LH (blue frame), E (green frame) and B (yellow frame). First column represents the fortnightly averaged DDM vs river discharge, the second column DDM vs tidal range (with distinct symbols according to its sign of variation : > between neap to spring and < spring to neap tide phase), and the third column DDM vs daily maximum wave Hs. Large symbols are used to represent DDM averaged over successive ranges of forcing values.

The variability observed around the trend induced by each forcing is largely explained by the other forcing effects. In fact river discharge presents the smallest temporal variability of the three considered forcings and thus its effects on DDM are likely to be blurred by forcings presenting higher temporal variability. Even if tidal currents are stronger on spring tides, model results demonstrate that counter-intuitively siltation in dredged areas is also higher during spring tide, probably because sediment transport is intensified globally. For example, at 500 $m^3.s^{-1}$ the average DDM in *zone E* is 10 kt/day but it can reach 35kt/day during spring tides.

4.3.2 Tide effect

Graphs b, e and h of Figure 7 focus on the tide induced variability. On these 3 graphs spring to neap (s2n) and neap to spring (n2s) tidal phases are plotted distinctly. Interestingly, a counter clockwise hysteresis is observed for the DDM of all three areas and especially in *zone B* and E where tidal currents are stronger than in *zone LH*. These model results also demonstrate that counter-intuitively siltation in dredged areas is higher on spring tides when currents are larger, because sediment transport is intensified globally.

Dredged sediment in *zone LH* stays very muddy during the neap/spring cycle with a slightly higher mud content for intermediate tidal range (+10%), while in *zone E and B*, the mud fraction in dredged sediment can vary up to 40% at a fortnightly scale. The maximum mud fraction in *zone E* is observed during the s2n phase when tidal range is about 4 to 5 meters, while in *zone B* the mud fraction is maximum for the smallest tidal range.

4.3.3 Storms effect

In the bay of Seine, during stormy conditions winds and waves are so strongly correlated that it is not possible to study their respective effect using the realistic retrospective simulation (Figure 8). In fact high wind speed, in particular from west, are associated with high wave conditions. Therefore storm effects are analyzed in two steps, i/ by analyzing the 10 years hindcast simulation considering wave Hs as the indicator of stormy conditions and ii/ by using a theoretical simulation in which wind could contribute to wave generation, but was not accounted for in the momentum equation: by this way, there was no effect of wind on circulation.
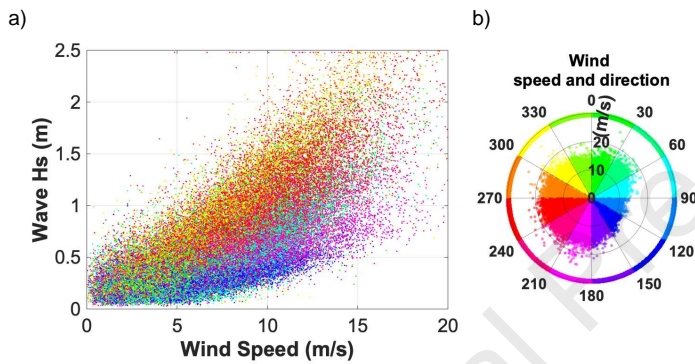

Figure 8 : a).Wind and waves correlation during the simulated period. b) Wind speed and direction during the simulated period. Waves and wind data where respectively extracted at zone V and point W specified on Figure 2 (cf. section 3.4).

Storms affect *zone LH and E* which are directly exposed to waves. In these two zones, waves appear to increase dredging in a non-linear way (Figure 7.c and f). The wave effect is more spectacular in *zone LH*, where for instance the DDM associated with 2 m waves is 4 times higher than with 1 m waves while the corresponding ratio is only 2 for *zone E*. Such non-linearities suggest that a unique storm is likely to generate intense dredging requirement, but the detailed infilling process when the storm is passing by was not investigated, being out of the scope of this study.

In *zones LH* and *E*, the dredged sediment nature also varies with wave height: mud fraction decreases with wave height. This feature is particularly visible at E, where the respective contributions of sand and mud are more balanced.

Wind effect

A specific simulation of the hydrological year august 2017 to august 2018 was set up using the *QCD* procedure. In this test case, wind effect on waves generation was considered so that waves conditions are the same as in the *QCD* run, but wind effect on circulation was not. The comparison of these two simulations enables to study the impact of wind induced circulation on dredging. Results of this test case present a significant increase in *zone E* where dredged masses are 57% larger without wind-induced circulation (Figure 9), corresponding to a 70% increase of dredged mud and 33% increase of dredged sands. Interestingly, these differences are all the more important as wind speed increases,

demonstrating the importance of wind induced circulation on sediment dynamics. Given the correlation between westerly winds and waves conditions it is plausible that these winds enhance flood currents and thus favor upwards and northward fine sediment transport. This is coherent with Le Hir et al. (1985) who demonstrated that in the eastern Bay of Seine, westerly winds induce a northern flow component around *zone E* (but probably not in *zone LH* which is located right south of the coast). This additive northward component hinder mud deposition in *zone E*. No significative changes were observed in *zone B* dredging.
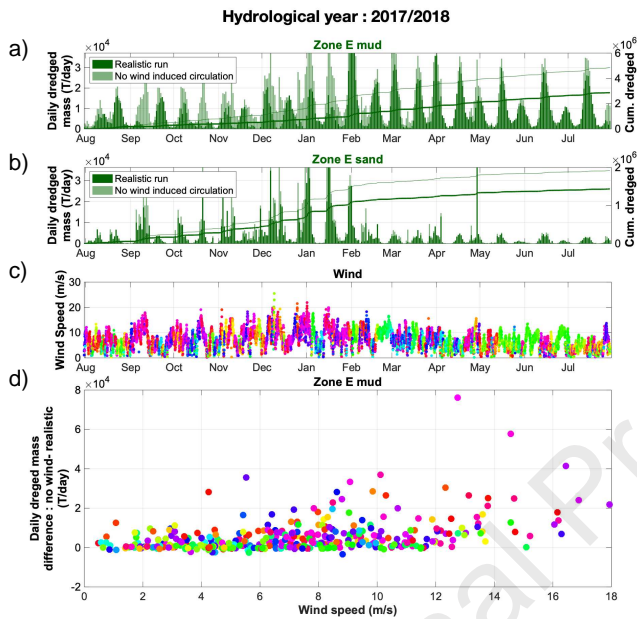

Figure 9 : Effect of wind-induced circulation on dredged masses during the hydrological year 2017-18. (a) daily and cumulated dredged mud in zone E, computed with (dark green) or without (light green) wind effect on circulation; (b) daily and cumulated dredged sand in zone E, computed with (dark green) or without (light green) wind effect on circulation; (c) wind speed and direction (color, same code as in Figure 8.b);. d) difference between total DDM computed in zone E without and with wind effects on circulation, versus wind speed and direction (color).

Finally, the three studied dredged areas present three contrasted sensitivities to the main forcing:

- *Zone LH* appears to be primarily affected by waves,
- *Zone E* dredging is affected by all forcings in terms of mass and sediment nature,
- *Zone B* seems to be mainly related to tides (tidal range and phase of spring/neap tidal cycle).

4.4. Distinctive responses of mud and sand dredged masses to hydro-meteorological forcings

To further analyze DDM variabilities, mud and sand are being studied separately : Mud (resp. sand) dredging designates the muddy (resp. sandy) part of the dredged quantities. For each zone DDM are averaged according to different ranges of each of the three studied forcings. In relevant cases, second order polynomial regressions between each DDM and each of the three forcings - river discharge, n2s and s2n tides, and waves (including wind effects) - are established separately for sand and mud (Figure 10). Aside from the polynomial regression, it is interesting to focus on the associated coefficient of determination (R^2) to have a qualitative insight on the effect of the considered forcing on DDM (Table 1).
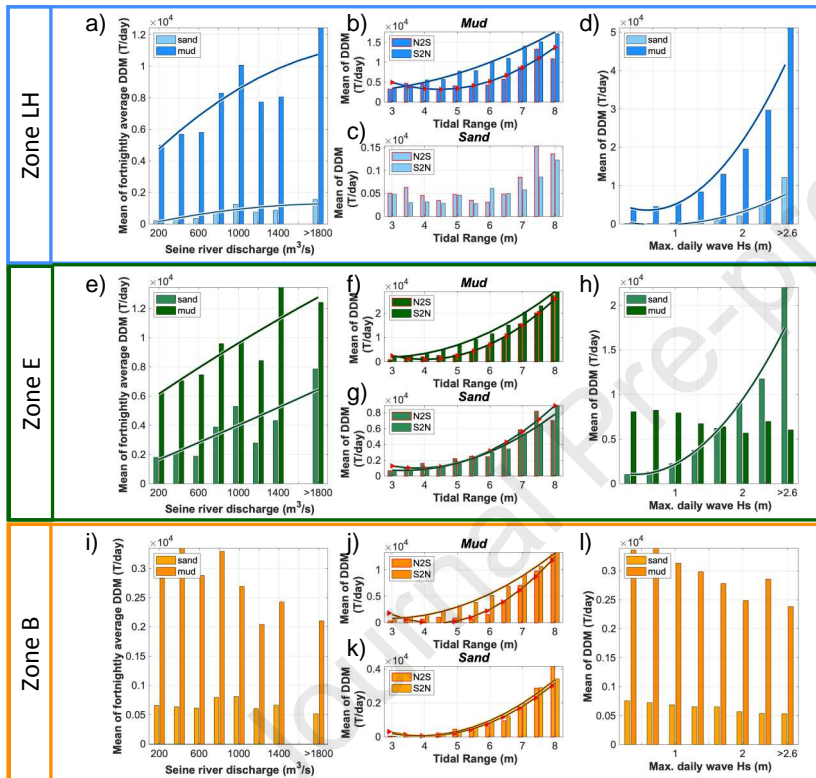

Figure 10 : Relations between daily dredged masses and forcing using the same layout as figure 7. Bars represent the DDM of sand (light color) and mud (dark color), averaged for different ranges of the three forcings (abscissa): river discharge, tidal range and wave intensity. Lines represent the polynomial regression over the whole data set (i.e. not the class-averaged DDM represented by the bars). Polynomial regressions are not represented when the associated coefficient of determination R^2 is close to zero (table 1).

4.4.1 *Zone LH*

In *zone LH*, correlations between maximum daily wave Hs and DDM demonstrate that theoretically waves explains 42% and 43% of DDM variability for mud and sand respectively. This representation also highlights that sand dredging at LH only occurs under stormy conditions. High river discharges slightly increase dredging needs but in this case the polynomial regression only explains 12% and 15% of DDM variability for mud and sand respectively. Given the shape of the correlation and the uncertainties associated with the higher river discharge classes, barplots of Figure 10.a show that DDM at LH does not vary with the river flow below 600 m³.s⁻¹, but increases significantly above, potentially revealing

two regimes of sediment dynamics in the vicinity of *zone LH* (*cf.* discussion in section 5). Tides only contribute to the variability of mud DDM, but in a lesser extent (R^2=0.08).

4.4.2 *Zone E*

In *zone E*, the second line of Figure 10 illustrates that sand and mud DDM present a similar sensitivity to river discharge but distinctive response to tidal range and waves. On this site, both sand and mud dredging increase almost linearly with river discharge, the associated regressions explaining almost 20% of DDM variabilities. Dependencies to tidal range and in particular the distinction between n2s and s2n period is interesting on this site as it demonstrates that sand dredging increases with tidal range similarly during s2n and n2s while mud dredging presents an hysteresis. Regressions between DDM and tidal range explain respectively 60% and 13% of mud and sand dredging variability, proving that mud deposition in *zone E* is mainly related to the tidal dynamic. Regarding waves effect on DDM at *zone E*, this analysis shows that waves are the main driver of sand accretion as the regression explains 40% of sand dredging variability. On the contrary, mud dredging appears to be independent of wave conditions but as shown in the previous section this might be due to the circulation induced by winds (accompanying wave episodes) which transport and maintain in suspension the mud eroded by waves.

4.4.3 *Zone B*

In *zone B*, DDM variabilities of both sand and mud appear to be mainly explained by the tidal range variations. The regressions between DDM and tidal range (s2n and n2s) explain almost 75% of both mud and sand DDM variabilities. Also, as observed in *zone E*, sand dynamic affects dredging similarly in s2n and n2s phases, while mud DDM presents an hysteresis. Otherwise no significant correlation between DDM and both river discharges and waves conditions are demonstrated (Table 1). Nevertheless, bar plots show that increases in river discharge or wave condition tend to decrease mud DDM.

Table 1 : Coefficient of determination R^2 associated to the second order polynomial regression between DDM and river discharge, tidal range and wave H_s. Regression are shown on figure 10. R^2 associated to tidal range is the average of the R^2 associated to n2s and s2n polynomial regressions.

		River Discharge	Tidal Range	Waves
Zone LH	*mud*	0,12	0,08	0,42
	sand	0,15	0,00	0,43
Zone E	*mud*	0,20	0,62	0,00
	sand	0,18	0,13	0,40
Zone B	*mud*	0,02	0,73	0,00
	sand	0,00	0,74	0,00

4.5. Toward a quantification of daily dredged masses: parametric model set up

When the coefficients of determination of the polynomial regressions set up in the previous section are not too low, it is conceivable to describe DDM (resulting from the process based model) as a polynomial function of the related forcing. Such a parametric model remains dependent on the validation and predictive capacity of the process-based model, but can be interesting from an operational point of view, as it can provide straightforwardly some quantification of dredging needs, without running the process-based model. In addition it would be likely to be used by stakeholders or by port authorities, without any required skill for running sophisticated models. According to the coefficients of determination listed in table 1, such a modeling exercise was attempted for *zones E and* B, but for conciseness purpose only zone E is presented hereafter.

For mud dredging in *zone E,* a first regression is fitted between DDM_{mud} and TR, distinguishing *n2s* and *s2n* phases. Then residuals are correlated to river discharge, following a second order polynomial function. The resulting parametric model writes:

$DDM_{mud} = 1.56*10^6 \ TR^2 - 1.25*10^7 \ TR - 0,23 \ Q^2 + 4.49*10^3 \ Q + 2.37*10^7$ during n2s phase

$DDM_{mud} = 9.78*10^5 \ TR^2 - 5.34*10^6 \ TR - 0,23 \ Q^2 + 4.49*10^3 \ Q + 6.71*10^6$ during s2n phase

where Q is the fortnightly averaged river discharge.

Regarding sand dredging in *zone E*, it appears that dredging is more sensitive to waves than to tidal range (with R^2 of 0.4 and 0.13). However the regression with tide is so clear (Figure 10.f and g) and the tidal forcing is so periodic and predictable that tide was selected as the first forcing to define the regression with. Here too, the two phases of the hysteresis have been considered apart. Then the residual (difference between the initial DDM and the approximated tide-induced DDM) is correlated to the wave index (representative H_s in the mouth). Last, the new residual is correlated to the third forcing, here river discharge. The full parametric model can be expressed:

- during neap to spring tidal phase:

$DDM_{sand} = 4.47*10^5 \ TR^2 - 3.38*10^6 \ TR + 3.44*10^6 \ H_s^2 - 2.89*10^6 \ H_s - 0.42 \ Q^2 + 531 \ Q + 5,99*10^6$

- during spring to neap tidal cycle:

$DDM_{sand} = 3,25*10^5 \ TR^2 - 2.16*10^6 \ TR + 3.44*10^6 \ H_s^2 - 2.89*10^6 \ H_s - 0.42 \ Q^2 + 531 \ Q + 4,13*10^7$

where H_s is the representative wave significant height. Figure 11 presents the performance of this parametric model.
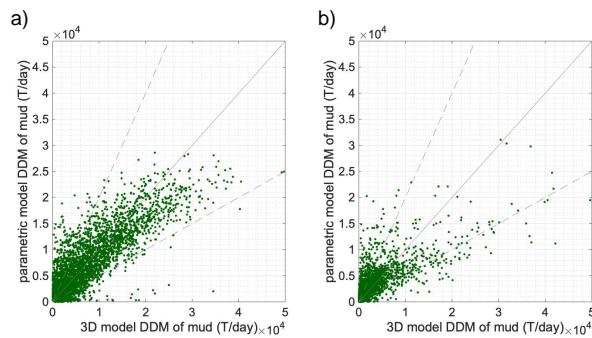
Figure 11 : Daily dredged masses of mud (a) and sand (b) at zone E computed with the parametric model vs total DDM provided by the process-based model, for the 9 simulated years.

On Figure11, targeted results are represented by the line 1/1, while dashed lines represent the limits between which the parametric model restitutes the results of the process-based model within a factor 2. The parametric model performs relatively well in both cases although large DDM values tend to be underestimated. It is reminded that possible effects of transitory stages of each forcing, as well as their history, are not accounted for in the proposed simple parametric model. The underestimation of large DDM can come from the impossibility for the model to account for i/ effects of cumulated intense forcing in relation with seasonal trends and ii/ nonlinear DDM increase when several influent forcings occur simultaneously. To tackle with interactions between hydro-meteorological forcings, a multivariate nonlinear analysis should be better appropriate, but is out of the scope of the present study.

4.6. Weight of each forcing at the annual time scale

Knowing the variability of dredging activity in the Seine Estuary, it is interesting to assess how much each forcing contributes on average to the annual cumulated dredged masses, when its own probability distribution is accounted for.

Regarding the Seine River discharge effects, Figure 12.a shows that even if dredging in *zones LH* and *zone E* increases with the Seine River discharge, almost 70% of dredging is achieved with moderate discharge between 100 and 700 $m^3.s^{-1}$. Nevertheless due to the sensibility of these two sites to high river discharges it appears that discharges above 700 $m^3.s^{-1}$, observed 20% of the time, induce 30% of dredged masses over a long period (here 10 years).

While Figure 10 illustrated the strong relationships between dredging in *zones E* and *B* and tidal range, Figure 12.b shows that these relations have an important impact over the whole simulated period, all the more that the tidal amplitude distribution is not Gaussian. Almost ±70% of dredging are executed during spring tides with tidal range higher than 6 m which corresponds to 40% of time. In *zone LH*, even if the relation with tidal range is not so pronounced, ±50% of dredging is achieved during these 40% of time.
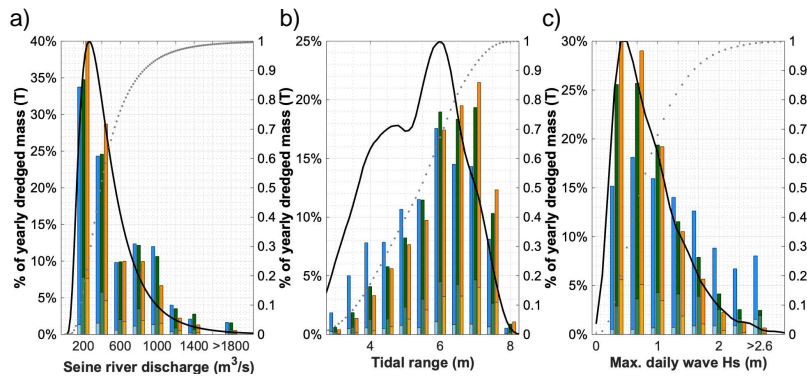
Figure12 : Total distribution of dredged masses of sand (light colors) and mud (dark colors) versus hydro-meteorological forcings : a) river discharge, b) tidal range and c) maximum daily wave H_s, over the 10 years simulated period. Colors represent the dredged zone : LH in blue, E in green and B in yellow. The probability density function of each forcing during the simulated period is represented as a solid black line and the associated cumulative density function as a dashed gray line(right axis).

Concerning the wave impact on the long-term dredging activity, results presented on Figure 12.c highlight the major role of waves on *zone LH* dredging. Actually almost 60% of dredging activity is due to waves higher than 1.3 m which are observed only 20% of time. In *zone E* wave impact is lower but still 30% of dredging activity is due to these stormy periods. Furthermore, this representation illustrates the independence of dredging in *zone B* to high waves, as the distribution of DDM exactly follows the probability density function of waves.

4.7. Inter-annual variability

As the storm probability and the hydrological cycle are likely to vary along successive years, it is interesting to focus on the interannual variability. In fact yearly dredged masses variability can exceed 50 % during the simulated period (Figure 4). For example in *zone E,* 4.5 MT were dredged during the hydrological year 2014/2015, but only 2.8 MT in 2010/2011.

To understand these interannual variabilities, the 9 hydrological years represented on Figure 5 were characterized by their annual mean river discharge, which provides an indicator of the flood intensity, and by the percentile 95 of wave H_s to represent the intensity/frequency of the storms. Figure 13 illustrates the variability of dredged masses in the 3 zones as a function of these indicators. The yearly-averaged Seine River discharge vary up to ±40% around its average of 488 $m^3.s^{-1}$ during the 9 hydrological years. Storms also present an important variability, 40 % for the percentile 95 of wave H_s.
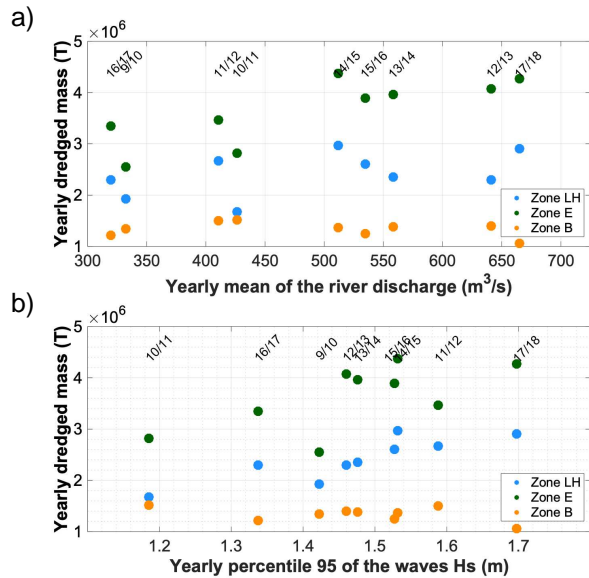
Figure 13 : Interannual variability of hydrometeorological forcings and yearly dredged masses for the 9 hydrological years from august 2009 to august 2018. Hydrometeorological forcings are characterized by the yearly mean river discharge (a) and the yearly percentile 95 of the wave H_s (b). Zone LH, E and B are represented using blue, green and orange resp. Hydrological years are indicated at the top of each figure, using the last digits of concerned year (for instance11/12 for the year mid-2011 / mid-2012).

In *zone LH* the important role of storm is highlighted as the highest yearly percentile 95 of waves $H_s$are associated to the highest yearly dredged mass (Figure 13.b). At *zone E*, the highest annual dredged masses are associated with the highly energetic years with important flood and storms. Previous results indicated that the variability of dredging in *zone B* was few related to waves and river discharge. However, it is interesting to note that during the year 2017-2018 which is the most intense year for both river discharge and waves conditions, dredging in *zone B* is minimum, in accordance with the slight DDM decrease in response to both river discharges and wave conditions observed on Figure 10.

5. Discussion

5.1 Performance of the modeling exercise

Dredged masses were evaluated by using a process-based model and assigning a navigation depth in specific areas, as in reality. This means that theoretically there is no specific parameter added to simulate dredging. The validation of dredged quantities (both masses and sediment composition) constitute an additional validation of the global hydro-sedimentary model.

In the case of the Seine Estuary, dredging simulations are actually validated, except for the sand extracted in one of the 3 major areas of dredging (*zone B)*. On this site, the simulated sand mass dredged appears to be 3 times smaller than *in-situ*, and does not vary seasonally although Rouen port authority observes an increase in winter. Actually this concentrated area of deposition in the navigation channel is likely to be nourished by the so-called Northern Channel, north of the northern submersible dyke (Figure 1), which communicates with the navigation channel through a breach very close to the dredging location. This Northern Channel is characterized by flood dominance and an eastward sand transport (*e.g.* Le Hir et

al., 2001). We think that the discrepancy between model and field observations could come from the crude resolution of our model in this area characterized by strong bathymetric gradients. However, the difficulty to simulate sand deposition in this area was also reported by Walther et al. (2015) who used a finite element model and a computational grid with higher resolution.

Regarding the methodology for studying the variability of dredging needs and its relation with forcing, an alternative strategy could have been chosen. For instance and for the sake of simplicity, series of short term runs with specific tide, wave, wind and river discharge conditions, possibly steady, could be processed. But such simulations would have been far from reality, as nonlinear effects of forcing addition and effects of transitional hydro-meteorological environments are likely to strongly influence sediment transport and dredging needs.

The 10 years duration of the runs allows to look for some effect of the morphological change on dredging needs. This has not been investigated so far, and any variation of dredged quantities on the long term should be interpreted cautiously, because of a possible consequence of the initial sediment condition. For instance, in *zone E*, the increase of dredged masses along the first 5 years for both sand and mud (Figure 4) can be induced by a change of surficial sediment in the surroundings. These features may also hinder the interpretation of the inter-annual variability as developed in section 4.7.

5.2 Links between dredging and sediment processes

A number of dredging results are straightforwardly linked to sediment processes, which are different for sands and mud.

Sand deposition is mainly controlled by the divergence of horizontal fluxes. In a macrotidal environment, tidal asymmetry may play an important role. Such process has been evoked for *zone B* right upstream the northern channel, and is clearly relevant for sand dredging in *zone E*, where a strong gradient of tidal residual sand transport tendencies, computed as the integration of u^5 along a tidal cycle, is predicted (Le Hir et al., 2001): upstream *zone E*, the residual flow and sediment transport is clearly seawards, as a result of the submersible dykes, while downstream the trend of residual sediment transport is negligible. Net deposition results in between, in deeper parts that correspond to the maintained navigation channel, in *zone E*. The process may be reinforced by the estuarine density-induced circulation which takes place in the same area on high river discharge (Schulz et al., 2018). The latter process explains the positive correlation of sand deposition with river discharge illustrated in Figure 10.e.

Muddy particles have a much lower settling velocity so that their transport in suspension lasts longer. As a result, mud transport is more influenced by wind-induced currents: this is clearly illustrated by Figure 9 which shows that when the effect of wind on circulation is neglected, although there is no significant difference on sand deposition in *zone E* after stormy periods, mud trapping is different in the same area: even if resuspension remains strongly controlled by waves, when wind-induced circulation is accounted for, it deviates the trajectory of mud particles and significantly reduces mud deposition in *zone E*.

Still because of the low settling velocity, mud transport is also influenced by time lags between resuspension and sedimentation. This results in a marked hysteresis during the tidal cycles, and at the time scale dredged masses are explored, during the fortnightly tidal cycle. On spring, resuspension is maximum, inducing an increase of concentration, and a maximum deposition in dredged areas few days later, as clearly shown on Figures 10.b, f and j for the 3 dredged zones. On the opposite, sand trapping (and dredging) is maximum on spring tides (Figures 10. c, g and k), in phase with higher resuspension.

A similar hysteresis cycle also occurs for the Seine estuary ETM as described by Grasso et al. (2018). Actually the ETM is located in the vicinity of *zone B* for intermediate river discharges, and close to *zone E* (then also closer to *zone LH*) for high river run off, but upstream of both zones during low river discharges. Then one can wonder whether the proximity of the ETM, with its own hysteresis, is likely to influence mud trapping in dredged areas. According to Figure 14, this seems the case. A quasi-linear correlation between mud DDM and ETM mass is observed for *zones E and B*, which is understandable as both quantities strongly depend on the tidal range. But the ratio between mud DDM and the ETM mass depend on the tide-averaged position of the ETM. For instance, at *zone E*, this ratio is much higher when the ETM is located downstream (yellow and red points on Figure 14.b), then close to the dredged zone. This feature is the simple explanation of the increase of mud dredging with river discharge demonstrated on Figure 10.d.

Similarly, at *zone B* (Figure 14.c) mud DDM is maximum when the ETM is located around pk355, in the vicinity of *zone B*, and minimum when the ETM is downstream. Regarding *zone LH*, the increase of mud DDM is also clear when ETM is downstream (high river discharge , in Figure 10.a), while DDM seems independent of the ETM mass in other cases (Figure 16.a).

In conclusion, the presence of the ETM seems to impact mud dredging, all the more that the simulated ETM mass is in the same order of magnitude as total dredging in only one day for all zones: about 60 000 tons on spring tide, if we except largest mud DDM in *zone LH* which are generated by waves (Figure 14.a).
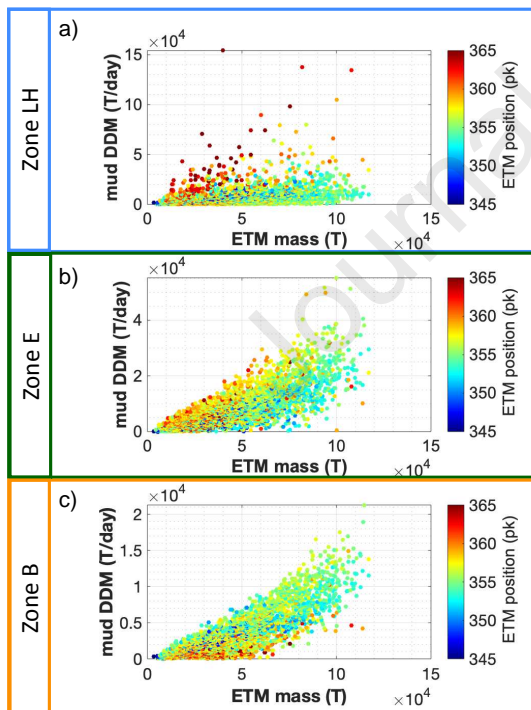

Figure 14 : Relation between the ETM (daily maximum mass and daily median position) and mud DDM simulated on the three zones: a) zone LH; b) zone E ; c) zone B. Position units (pk) are distance from Paris (in km), represented on Figure 1.

5.3 Role of forcing concomitance

In section 4.3.3, we investigated the co-occurrence of high waves and influent winds on dredged masses. Actually, these two forcings are somehow correlated, and their common effect is quite different from the effect of each forcing. Among the dominant forcings, another concomitance may occur: the temperate and oceanic climate in the region of the Seine Estuary often generates strong rains in the watershed, accompanying storms with westerly winds and waves in the Bay of Seine. Results prove that when river discharge is high, waves are more often high, and these occurrences correspond to maximal DDM in *zone E*, demonstrating an effect of the forcing concomitance on dredging. On the other hand, a reduction of DDM is observed at *zone B* more probably due to the downwards shift of the ETM than to a reduction of sediment trapping during storms.

6. Conclusions

This study demonstrates the capacity of the Mars3D-Mustang-WWIII process-based model of the Seine Estuary, developed by Grasso et al. (2018), Mengual et al. (2020*)* and fitted in the frame of this study, to reproduce the Seine Estuary functioning and in particular its maintenance dredging over 10 years. In fact, the model which considers real forcings (river discharge, tides, wind and waves) simulates a realistic ETM and reproduces the 3 main features of dredging:

- i/ continuous dredging needs;
- ii/ localization at the estuarine mouth, with more than 90% of dredging concentrated in the three areas discussed in section 4 and
- iii/ dredged sediment composition varying with space and time, as the model is considering 5 different sediment classes.

Two types of simulations were conducted, considering two different dredging thickness. The level of validation is similar for both runs, but the realistic one (dredging thickness of 50 cm) is in better agreement with field data. Differences between the realistic and *QCD* run (dredging thickness of 1 cm) demonstrated that the morphological effect of each dredging operation are not affecting dredged quantities significantly.

Depending on their exposure to waves and currents, the three studied dredging zones have different sensibilities to the considered forcings. Dredging requirements in *zone LH* are mainly induced by storms. In *zone E*, sand accretion is primarily related to storms but also to river discharges and tidal range. However on this same site mud deposition is firstly related to tidal conditions and then to river discharges, but is independent of storms. In order to distinguish wind and waves contributions, which are correlated in the Seine Estuary, a theoretical simulation that considers wind effect on waves but not on circulation was set up. Comparisons of this theoretical test with the regular run over one year demonstrates that during storms, resuspended mud is transported out of *zone E* by the wind induced circulation, explaining a low effect of storms on mud dredging in this area, in opposition to sand dredging. The nice relationships between DDM and forcings allow us to propose a parametric polynomial model which straightfordly gives a reasonable estimation of the daily dredging needs in response to forcing values. In *zone B,* mud deposits appear to be mainly induced by tidal dynamic, while sand accretion is underestimated by the model.

In relation with the low mud settling velocity and the resulting delay between erosion and siltation, mud dredging on the three zones presents a counter clockwise hysteresis in response to the tidal range fortnightly cycle. Also these dredging zones which are in the vicinity of the ETM are affected by its dynamic. On each site mud DDM increases when the ETM is nearby, which explains the mud dredging increase (resp. decrease) in *zones LH and E* (resp. *zone B*) associated to high river discharges that shift the ETM downstream. Moreover, in *zone E and B* which are in the direct vicinity of the ETM, dredging increases almost linearly with the ETM mass which constitutes a major source of fine sediment.

Regarding sand dredging in zones exposed to waves (*zone LH and E*), it appears to increase in a quadratic way with wave H_s, in analogy with the resuspension rate. However, sand deposition in dredged areas may also be dependent on the river discharge, as the latter influences the location of the near bottom density-induced circulation which takes place in estuaries.

Overall, this analysis shows that dredging increases with the resuspension induced by each forcing. It demonstrates that at annual scale most of the dredging requirements are induced by the highest intensities of the considered forcings. Finally, given each forcing temporal variabilities and the potential co-occurrences of high river discharges and storms,

dependencies between dredging and hydrometeorological forcings can lead to 50% interannual variability of dredging requirements.

In terms of perspective, the model is being used (1) to analyze the role of maintenance dredging in the physical functioning of the Seine Estuary, regarding suspensions, surficial sediment evolution and morphological trends, and (2) to test the effect of alternative dredging strategies (e.g. use of different dumping site). The methodology we set up for the Seine Estuary in order to predict dredging requirements according to natural forcing could be applied in other areas submitted to extensive maintenance dredging.

Bibliography

ARTELIA, 2018. Réhabilitation des vasières de la Seine: Mise en place d'indicateurs de suivi des évolutions morpho-sédimentaire 33.

Avoine, J., 1995. Synthese des connaissances sur l'estuaire de la seine. Rapp. d'études IFREMER 156.

Avoine, J., Allen, G.P., Nichols, M., Salomon, J.C., Larsonneur, C., 1981. Suspended-sediment transport in the Seine estuary, France: Effect of man-made modifications on estuary-shelf sedimentology. Mar. Geol. 40, 119–137. https://doi.org/10.1016/0025-3227(81)90046-3

Blanpain, O., 2009. Dynamique sédimentaire multiclasse : de l'étude des processus à la modélisation en Manche.

Dalrymple, R.W., Zaitlin, B.A., Boyd, R., 1992. Estuarine facies models : conceptual basis and stratigraphic implications. J. Sediment. Petrol. 62, 1130–1146. https://doi.org/10.1306/D4267A69-2B26-11D7-8648000102C1865D

Dam, G., Poortman, S.E., Bliek, A.J., Plancke, Y., 2013. Long-term modeling of the impact of dredging strategies on morpho- and hydrodynamic developments in the Western Scheldt. 20th World Dredg. Congr. Exhib. 2013 (WODCON XX). Art Dredging. Brussels, Belgium, 3-7 June 2013 739.

Delinares, M., Walther, R., Schaguene, J., Cyrielle, C., Hamm, L., 2015. Development of an hydro-sedimentary 3D model with sand-mud mixture - calibration and validation on 6 years evolution in the Seine Estuary 25–26.

Duclos, P.A., 2012. Impacts morpho-sédimentaires de l'extraction de granulats marins. Application au bassin oriental de la Manche.

Grasso, F., 2015. Numerical modelling of mixed-sediment consolidation 65, 607–616.

Grasso, F., Le Hir, P., 2019. Influence of morphological changes on suspended sediment dynamics in a macrotidal estuary: diachronic analysis in the Seine Estuary (France) from 1960 to 2010. Ocean Dyn. 69, 83–100. https://doi.org/10.1007/s10236-018-1233-x

Grasso, F., Verney, R., Le Hir, P., Thouvenin, B., Schulz, E., Kervella, Y., Khojasteh Pour Fard, I., Lemoine, J.P., Dumas, F., Garnier, V., 2018. Suspended Sediment Dynamics in the Macrotidal Seine Estuary (France): 1. Numerical Modeling of Turbidity Maximum Dynamics. J. Geophys. Res. Ocean. 123, 558–577. https://doi.org/10.1002/2017JC013185

Grasso, F. , Mengual, B., Le Hir, P., Walther, R., 2020. Rapport du projet Seine-Aval 6 Morphoseine – Modélisation de l'évolution morphosédimentaire de l'estuaire de la Seine. 74p.

IADC, 2011. Dredging In figures 2011. Internatioal Assoc. Dredg. Co. Annu. Rev.

Jonsson, I.G., 1966. WAVE BOUNDARY LAYERS AMD FRICTION FACTORS. Coast. Eng. Proc. 1. https://doi.org/10.9753/icce.v10.9

Landemaine, V., 2016. Érosion des sols et transferts sédimentaires sur les bassins versants de l'Ouest du Bassin de Paris : analyse, quantification et modélisation à l'échelle pluriannuelle. PhD Thesis, Univ. Rouen Normandy 235.

Lazure, P., Dumas, F., 2008. An external-internal mode coupling for a 3D hydrodynamical model for applications at regional scale (MARS). Adv. Water Resour. 31, 233–250. https://doi.org/10.1016/j.advwatres.2007.06.010

Le Hir, P., Cayocca, F., Waeles, B., 2011. Dynamics of sand and mud mixtures: A multiprocess-based modelling strategy. Cont. Shelf Res. 31, 135–149. https://doi.org/10.1016/j.csr.2010.12.009

Le Hir P., Silva Jacinto R., 2007. Currents, waves and tides: water movements. Booklet N°2 of the Seine-Aval programme, Quae ed., 31p.

Lemoine, J.-P., Le Hir, P., Grasso, F., 2020. Numerical Study of Sediment Transport in the Seine Estuary: Contribution of Dredging, in: Nguyen, K.D., Guillou, S., Gourbesville, P., Thiébot, J. (Eds.), Estuaries and Coastal Zones in Times of Global Change. Springer Singapore, Singapore, pp. 241–255.

Lemoine, J., Verney, R., Cayrol, C., Deloffre, J., Fisson, C., Grasso, F., Guézennec, L., Hamm, L., Landemaine, V., Lesourd, S., 2015. Fonctionnement hydro-sédimentaire de l'estuaire de la Seine. Fasc. Seine-Aval 3.3 64p.

Lesourd, S., Lesueur, P., Brun-Cottan, J.C., Garnaud, S., Poupinet, N., 2003. Seasonal variations in the characteristics of superficial sediments in a macrotidal estuary (the Seine inlet, France). Estuar. Coast. Shelf Sci. 58, 3–16. https://doi.org/10.1016/S0272-7714(02)00340-2

Liu, M., Zhang, H.W., 2019. Correction of the Artificial Influence on Dredging Volume in the Yangtze Estuary Deep-water Channel. IOP Conf. Ser. Earth Environ. Sci. 304. https://doi.org/10.1088/1755-1315/304/2/022004

Martelo, A.F., Trombetta, T.B., Lopes, B. V., Marques, W.C., Möller, O.O., 2019. Impacts of dredging on the hydromorphodynamics of the Patos Lagoon estuary, southern Brazil. Ocean Eng. 188, 106325. https://doi.org/10.1016/j.oceaneng.2019.106325

Mengual, B., Hir, P. Le, Cayocca, F., Garlan, T., 2017. Modelling fine sediment dynamics: Towards a common erosion law for fine sand, mud and mixtures. Water (Switzerland) 9. https://doi.org/10.3390/w9080564

Mengual, B., Le Hir, P., Rivier, A., Caillaud, M., Grasso, F., 2020. Numerical modelling of bedload and suspended load contributions to morphological evolutions of the Seine estuary (France). Int. J. Sediment Res.

Newell, R.C., Seiderer, L.J., Hitchcock, D.R., 1998. The impact of dredging works in coastal waters: A review of the sensitivity to disturbance and subsequent recovery of biological resources on the sea bed. Oceanogr. Mar. Biol. 36, 127–178.

Nguyen, D., Florence, L., pham van bang, D., Sylvain, G., Dan, N., Julien, C., 2012. Simulation of dredged sediment releases into homogeneous water using a two-phase model. Adv. Water Resour. 48, 102–112. https://doi.org/10.1016/j.advwatres.2012.03.009

Roland, A., Ardhuin, F., 2014. On the developments of spectral wave models: Numerics and parameterizations for the coastal ocean Topical Collection on the 7th International Conference on Coastal Dynamics in Arcachon, France 24-28 June 2013. Ocean Dyn. 64, 833–846. https://doi.org/10.1007/s10236-014-0711-z

Schulz, E., Grasso, F., Le Hir, P., Verney, R., Thouvenin, B., 2018. Suspended Sediment Dynamics in the Macrotidal Seine Estuary (France): 2. Numerical Modeling of Sediment

Fluxes and Budgets Under Typical Hydrological and Meteorological Conditions. J. Geophys. Res. Ocean. 123, 578–600. https://doi.org/10.1002/2016JC012638

Seity, Y., Malardel, S., Hello, G., Bénard, P., Bouttier, F., Lac, C., Masson, V., 2011. The AROME-France convective-scale operational model. Mon. Weather Rev. 139, 976–991. https://doi.org/10.1175/2010MWR3425.1

Soulsby, R., 1997. Dynamics of marine sands : a manual for practical applications.

Soulsby, R.L., Hamm, L., Klopman, G., Myrhaug, D., Simons, R.R., Thomas, G.P., 1993. Wave-current interaction within and outside the bottom boundary layer. Coast. Eng. 21, 41–69. https://doi.org/10.1016/0378-3839(93)90045-A

van Kessel, T., Vanlede, J., van Holland, G., 2015. Human versus natural mud fluxes in the Scheldt estuary: are they significant and if so, how can they best be optimised? Scheldt Estuary Phys. Integr. Manag. - Spec. Sess. 36th IAHR WORLD Congr. 28 June – 3 July, 2015, Hague, Netherlands 34–37.

Van Leussen, W., 1994. Estuarine macroflocs and their role in fine-grained sediment transport = Macrovlokken en hun bijdrage aan de slibtransporten in estuaria. Ministry of Transport, Public Works and Water Management, National Institute for Coastal and Marine Management (RIKZ), Den Haag.

Waeles, B., Le Hir, P., 2006. Simulation des activités de dragage et de leur impact sédimentaire à l'aide d'une modélisation morphodynamique de l'embouchure de la Seine 471–481. https://doi.org/10.5150/jngcgc.2006.046-w

Walther, R., Delinares, M., Hamm, L., Galichon, P., Scherrer., P., 2015. Développement d'un modèle numérique 3D morphodynamique de l'estuaire de la Seine, in: ECSA – Le Havre.

Wu, W., Lin, Q., 2014. Nonuniform sediment transport under non-breaking waves and currents. Coast. Eng. 90, 1–11. https://doi.org/10.1016/j.coastaleng.2014.04.006

Zhao, J., Guo, L., He, Q., Wang, Z.B., van Maren, D.S., Wang, X., 2018. An analysis on half century morphological changes in the Changjiang Estuary: Spatial variability under natural processes and human intervention. J. Mar. Syst. 181, 25–36. https://doi.org/10.1016/j.jmarsys.2018.01.007

Maintenance dredging in a macrotidal estuary: modelling and assessment of its variability with hydro-meteorological forcing

J.P. Lemoine[1*]; P. Le Hir[2]

[1] :   GIP Seine-Aval, Hangar C - Espace des Marégraphes, Quai de Boisguilbert, 76000 Rouen, France ; jplemoine@seine-aval.fr   (*corresponding author)

[2] :   IFREMER – DYNECO/DHYSED, Centre de Bretagne, 29280 Plouzané, France

Keywords

Seine Estuary - maintenance dredging - mud and sand transport - numerical model - hydrodynamic forcing

Highlights

- Maintenance dredging is simulated by a process-based model in a macrotidal estuary
- Dredging of sand and mud are related to hydro-meteorological forcings differently
- Dredging needs increase with resuspension either induced by waves or tidal currents
- Mud dredging is sensitive to the presence of an estuarine turbidity maximum
- Sand dredging varies with river discharge because of the estuarine bottom circulation
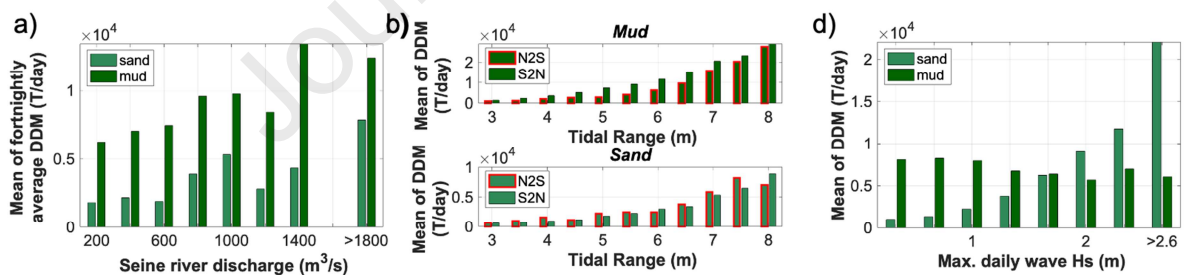
Highlights figure: Relations between Daily Dredged Masses (DDM) and forcings in a specific dredged zone ("Zone E") . Bars represent the DDM of both sand (light color) and mud (dark color), averaged for different ranges of forcing (abscissa) in response to river discharge (a), tidal range with distinct symbols according to its sign of variation : increasing tidal range (red border), decreasing tidal range (black border) for mud (f) and sand (g) and wave intensity (d). (Extract of figure 11)

Declaration of interests

☒ The authors declare that they have no known competing financial interests or personal relationships that could have appeared to influence the work reported in this paper.

☐ The authors declare the following financial interests/personal relationships which may be considered as potential competing interests:

Jean Philippe Lemoine   Pierre Le Hir :